# Electronic Supplementary Information

## Enhancement of ionic conductivity in Li argyrodite solid electrolytes with bromide and borohydride anions for all-solid-state batteries

Hyungeun Seo,[a] Yong-Jin Jang,[a] Jaeseong Yoo,[a] Ji-Hoon Han,[bc] Young-Su Lee,[b] Jae Yup Jung,[d] Soeun Lee,[d] Kyung-Woo Yi,[c] Young Whan Cho,[b] Woosuk Cho*[d] and Jae-Hun Kim*[a]

[a]School of Materials Science and Engineering, Kookmin University, Seoul 02707, Republic of Korea. E-mail: jaehunkim@kookmin.ac.kr (J.-H. Kim)

[b]Energy Materials Research Center, Korea Institute of Science and Technology, Seoul 02792, Republic of Korea

[c]Department of Materials Science and Engineering, Seoul National University, Seoul 08826, Republic of Korea

[d]Advanced Batteries Research Center, Korea Electronics Technology Institute, Seongnam, Gyeonggi 13509, Republic of Korea. E-mail: cho4153@keti.re.kr (W. Cho)

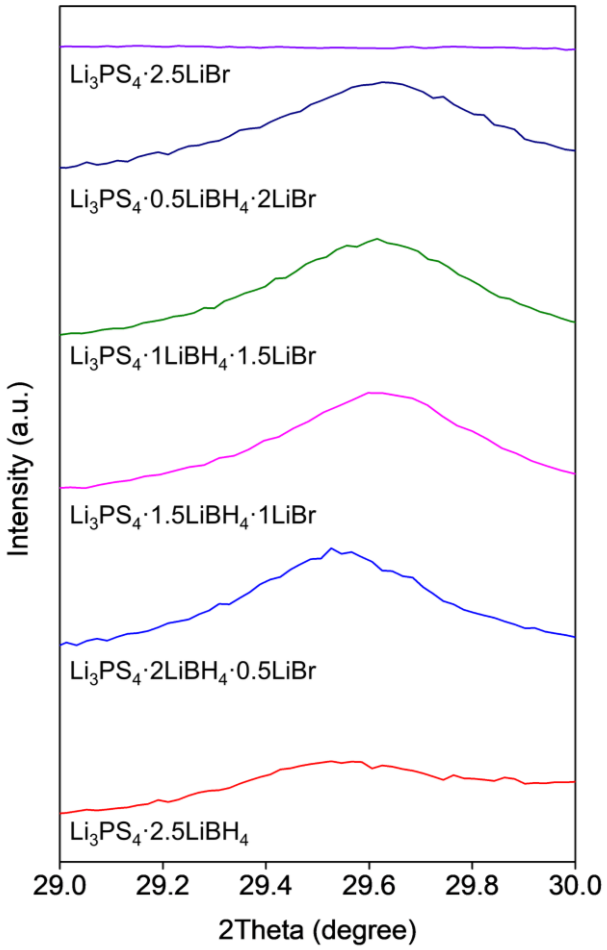


Fig. S1. Enlarged XRD patterns of the prepared solid electrolytes with the composition of $Li_3PS_4 \cdot (2.5–x)LiBH_4 \cdot xLiBr$.

Table S1. Isotropic temperature factor ($B_{eq}$) and isotropic displacement parameter ($U_{iso}$) for the Rietveld refinement of the prepared solid electrolyte sample ($Li_3PS_4 \cdot 2LiBH_4 \cdot 0.5LiBr$).
($B_{eq} = 8\pi^2 U_{iso}$)

| Atom | Site | $B_{eq}$ | $U_{iso}$ |
|---|---|---|---|
| Li | 48h(T5) | 5.8 | 0.073458 |
| P | 4b | 2.06 | 0.02609 |
| S | 16e | 2.64 | 0.033436 |
| S | 4d | 2.31 | 0.029256 |
| B | 4d | 2.31 | 0.029256 |
| Br | 4d | 2.31 | 0.029256 |
| S | 4a | 3.02 | 0.038249 |
| B | 4a | 3.02 | 0.038249 |
| Br | 4a | 3.02 | 0.038249 |
| H(B@4d) | 16e | 2.31 | 0.029256 |
| H(B@4d) | 16e | 2.31 | 0.029256 |
| H(B@4a) | 16e | 3.02 | 0.038249 |
| H(B@4a) | 16e | 3.02 | 0.038249 |

Rietveld refinement was performed using TOPAS v.5 software (Bruker AXS) over the 2θ range of 10°–70°. Because the limited quality of the XRD data did not allow us to refine the position of H in $BH_4^-$, the B–H bond length was fixed to 1.1 Å, the usual bond length of B–H obtained from XRD. Within the symmetry of F–43m, there are two possible orientations of $BH_4^-$, and we assumed an equal occupancy for the two orientations.

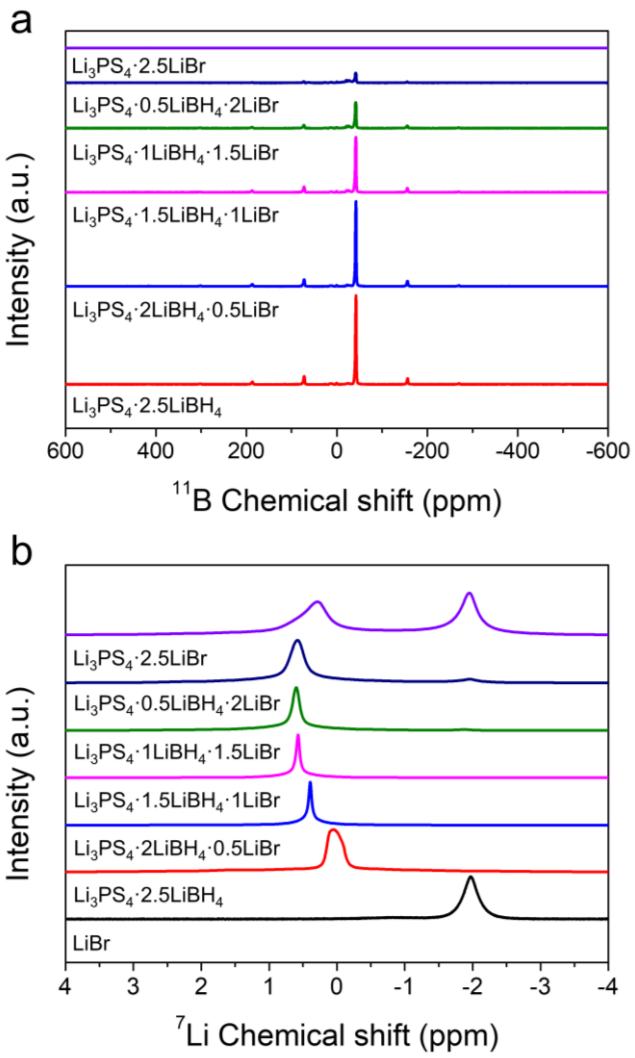


Fig. S2. (a) $^{11}$B and (b) $^{7}$Li solid-state MAS NMR spectra of the prepared solid electrolyte samples with the composition of $Li_3PS_4 \cdot (2.5–x)LiBH_4 \cdot xLiBr$.

For the $^{7}$Li solid-state MAS NMR spectra of the $x = 0.5$ sample ($Li_3PS_4 \cdot 2LiBH_4 \cdot 0.5LiBr$), the main peak is observed at 0.4 ppm, which is in good agreement with the previous report. When the $x$ value increases, the main peak position of the solid electrolyte samples shifts toward a higher frequency. This trend is observed as the amount of $LiBH_4$ in the argyrodite samples decreases. In the $x = 2.5$ sample ($Li_3PS_4 \cdot 2.5LiBr$), a peak at approximately –2.0 ppm is observed, attributed to the unreacted LiBr. This result is consistent with the XRD results. Moreover, when LiBr is added, as indicated by the XRD results, it increases the degree of crystallinity, which can sharpen the peaks in the $^{7}$Li solid-state MAS NMR spectra. However, when more than 1 equivalent of LiBr is added, unreacted LiBr appears, causing an uneven local magnetic field around the Li ions, which can broaden the NMR peaks.

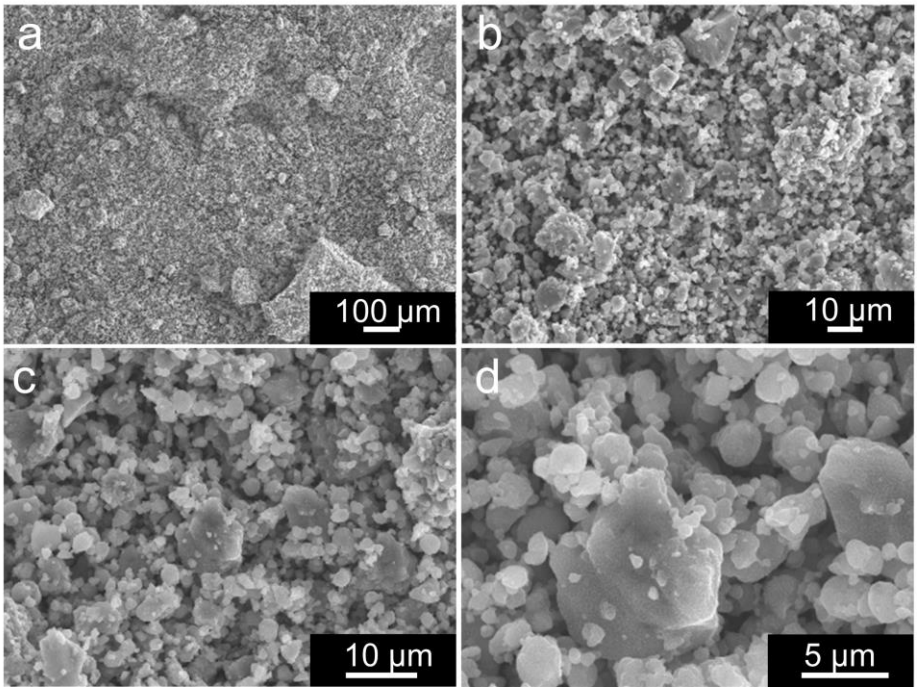


Fig. S3. FE-SEM images of the prepared solid electrolyte sample ($Li_3PS_4 \cdot 2LiBH_4 \cdot 0.5LiBr$) at different magnifications.

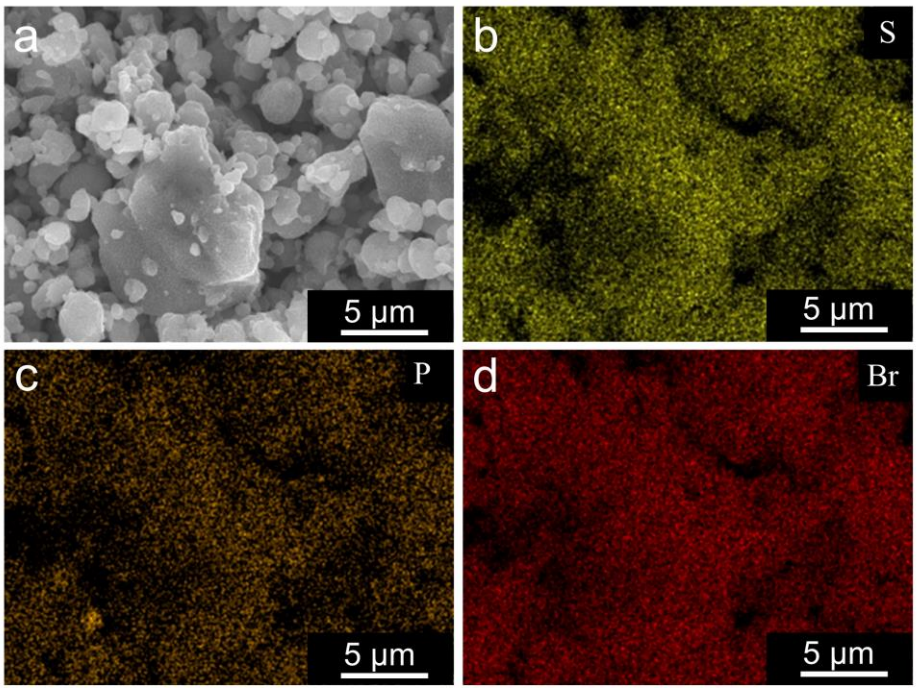


Fig. S4. (a) FE-SEM and (b–d) EDS elemental mapping images of the prepared solid electrolyte sample ($Li_3PS_4 \cdot 2LiBH_4 \cdot 0.5LiBr$).

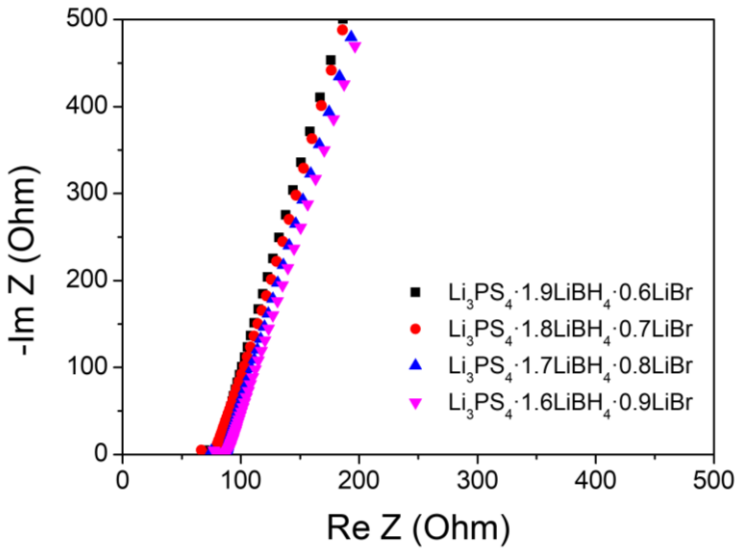


Fig. S5. Nyquist plots of the cells including the prepared solid electrolytes with the composition of $Li_3PS_4 \cdot (2.5–x)LiBH_4 \cdot xLiBr$ ($x$ = 0.6, 0.7, 0.8, and 0.9).

Table S2. Ionic conductivities of the prepared solid electrolyte samples.

| $x$ | Composition | Ionic conductivity (mS $cm^{-1}$ at 25°C) |
|---|---|---|
| 0.6 | $Li_3PS_4 \cdot 1.9LiBH_4 \cdot 0.6LiBr$ | 13.7 |
| 0.7 | $Li_3PS_4 \cdot 1.8LiBH_4 \cdot 0.7LiBr$ | 14.4 |
| 0.8 | $Li_3PS_4 \cdot 1.7LiBH_4 \cdot 0.8LiBr$ | 12.9 |
| 0.9 | $Li_3PS_4 \cdot 1.6LiBH_4 \cdot 0.9LiBr$ | 10.3 |

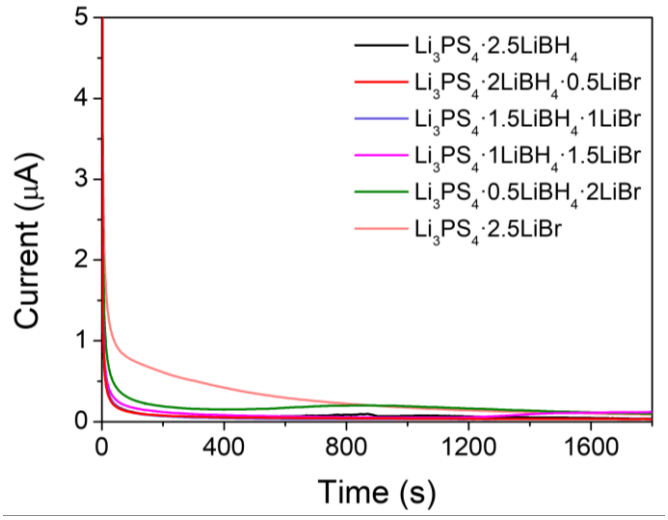


Fig. S6. DC polarization profiles of the prepared solid electrolyte samples with the composition of $Li_3PS_4 \cdot (2.5–x)LiBH_4 \cdot xLiBr$.

The resistance R is obtained from the measured DC polarization plot, and the conductivity of the samples can be calculated using the equation:

$$\sigma = \frac{t}{RA}$$

where t is the thickness of the sample and A is its area.

Table S3. Electronic conductivities of the prepared solid electrolyte samples with the composition of $Li_3PS_4 \cdot (2.5–x)LiBH_4 \cdot xLiBr$.

| *x* | Composition | Electronic conductivity (mS $cm^{-1}$ at 25°C) |
|---|---|---|
| 0 | $Li_3PS_4 \cdot 2.5\ LiBH_4$ | $8.8 \times 10^{-5}$ |
| 0.5 | $Li_3PS_4 \cdot 2LiBH_4 \cdot 0.5LiBr$ | $9.2 \times 10^{-5}$ |
| 1 | $Li_3PS_4 \cdot 1.5LiBH_4 \cdot 1LiBr$ | $7.4 \times 10^{-5}$ |
| 1.5 | $Li_3PS_4 \cdot 1LiBH_4 \cdot 1.5LiBr$ | $3.7 \times 10^{-5}$ |
| 2 | $Li_3PS_4 \cdot 0.5LiBH_4 \cdot 2LiBr$ | $3.1 \times 10^{-5}$ |
| 2.5 | $Li_3PS_4 \cdot 2.5LiBr$ | $1.5 \times 10^{-5}$ |

Table S4. Activation energy of the prepared solid electrolyte samples with the composition of $Li_3PS_4 \cdot (2.5–x)LiBH_4 \cdot xLiBr$. The activation energy errors across several trials are within ±0.5 kJ $mol^{-1}$.

| *x* | Composition | Activation energy (kJ $mol^{-1}$) |
|---|---|---|
| 0.5 | $Li_3PS_4 \cdot 2LiBH_4 \cdot 0.5LiBr$ | 28.8 |
| 1 | $Li_3PS_4 \cdot 1.5LiBH_4 \cdot 1LiBr$ | 29.6 |
| 1.5 | $Li_3PS_4 \cdot 1LiBH_4 \cdot 1.5LiBr$ | 29.8 |
| 2 | $Li_3PS_4 \cdot 0.5LiBH_4 \cdot 2LiBr$ | 32.8 |
| 2.5 | $Li_3PS_4 \cdot 2.5LiBr$ | 29.2 |

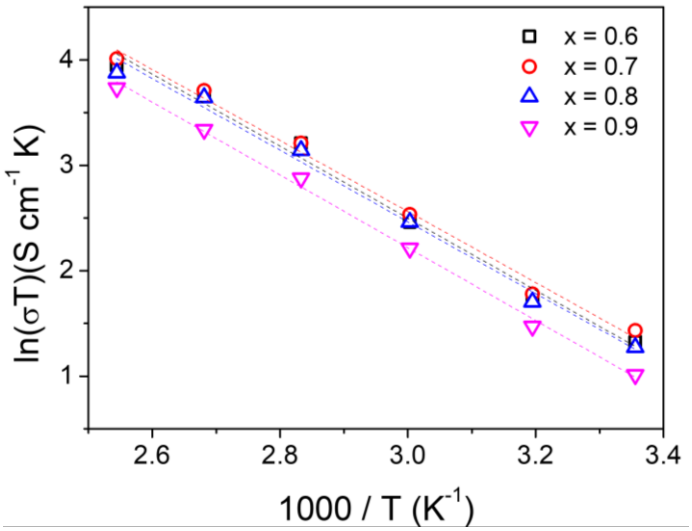


Fig. S7. Temperature dependence of ionic conductivities shown by the prepared solid electrolyte samples with the composition of $Li_3PS_4$·(2.5–*x*)$LiBH_4$·*x*LiBr.

Table S5. Activation energy of the prepared solid electrolyte samples with the composition of $Li_3PS_4$·(2.5–*x*)$LiBH_4$·*x*LiBr.

| *x* | Composition | Activation energy (kJ $mol^{-1}$) |
|---|---|---|
| 0.6 | $Li_3PS_4$·1.9$LiBH_4$·0.6LiBr | 28.3 |
| 0.7 | $Li_3PS_4$·1.8$LiBH_4$·0.7LiBr | 27.9 |
| 0.8 | $Li_3PS_4$·1.7$LiBH_4$·0.8LiBr | 28.3 |
| 0.9 | $Li_3PS_4$·1.6$LiBH_4$·0.9LiBr | 28.9 |

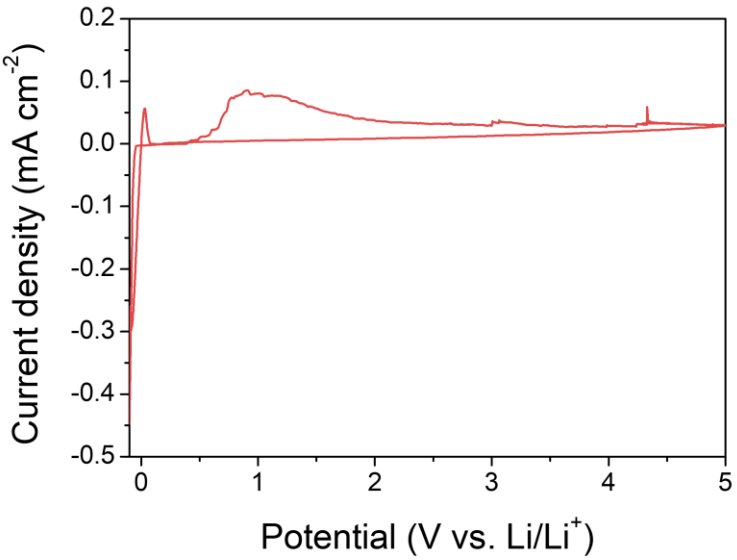


Fig. S8. CV curves of the Li/solid electrolyte/solid electrolyte-conductive carbon/SS cell measured at a scan rate of 1 mV $cm^{-1}$.

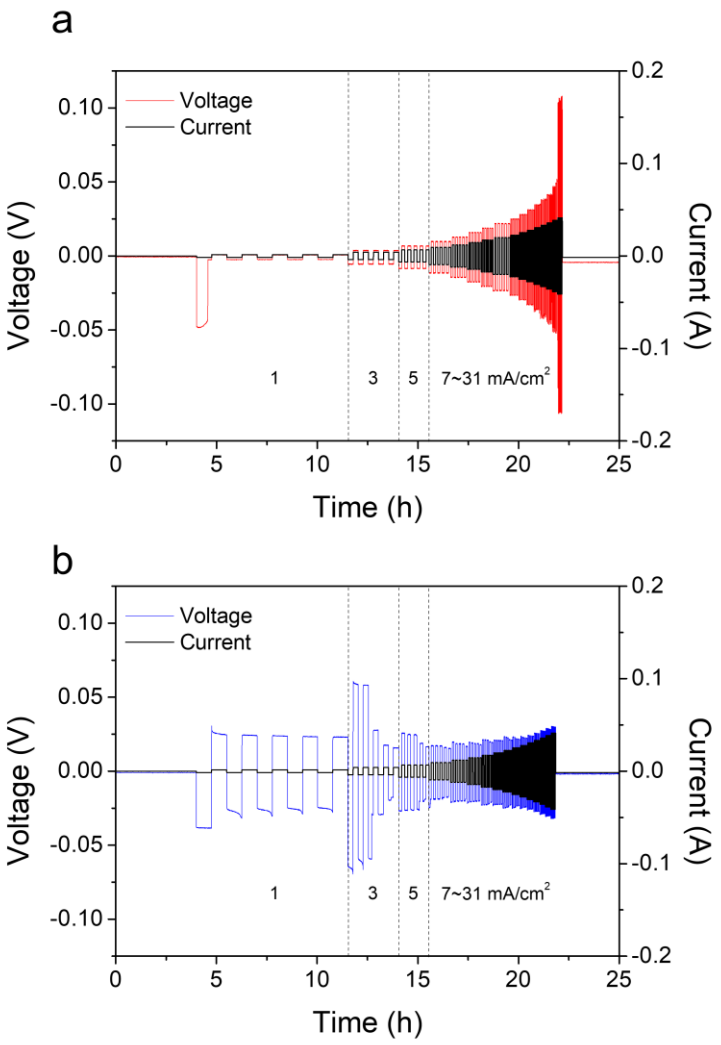


Fig. S9. Voltage profiles of the Li metal symmetric cells including the prepared solid electrolytes: (a) $Li_3PS_4 \cdot 2.5LiBH_4$ and (b) $Li_3PS_4 \cdot 2LiBH_4 \cdot 0.5LiBr$.

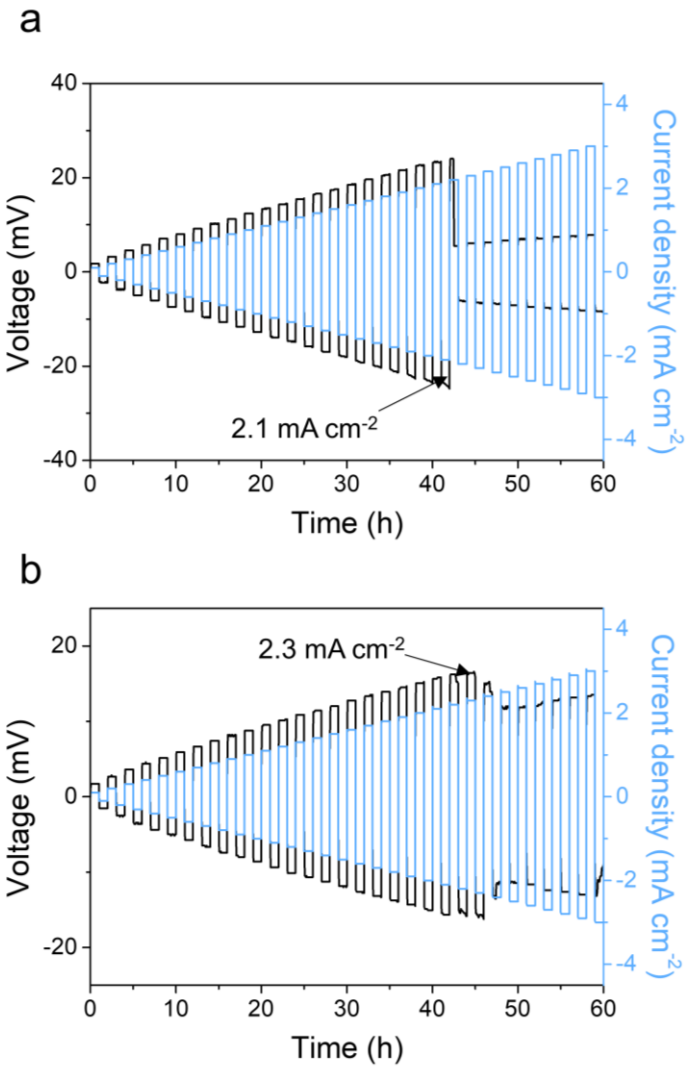


Fig. S10. Critical current density profiles using the time-constant mode: (a) $Li_3PS_4 \cdot 2.5LiBH_4$ and (b) $Li_3PS_4 \cdot 2LiBH_4 \cdot 0.5LiBr$.